ELSEVIER

Journal of Photochemistry and Photobiology A: Chemistry 116 (1998) 191–202

Journal of Photochemistry and Photobiology A:Chemistry

Photophysics of 4-dimethylamino cinnamic acid in different environments

Prakriti Ranjan Bangal, Sankar Chakravorti *

Department of Spectroscopy, Indian Association for the Cultivation of Science, Jadavpur, Calcutta 70032, India

Received 21 January 1998; received in revised form 6 April 1998; accepted 28 May 1998

Abstract

4-dimethylamino cinnamic acid (DMACA) has been studied by steady state and time-resolved fluorescence spectroscopy in different environments in order to get the information about its photophysics and photochemistry. Dual fluorescence in polar medium has been assigned to be arising out of delocalized excited state (DE) and twisted intramolecular charge transfer (TICT) state from different experimental and theoretical considerations. The computed excited state dipole moments in different twisted geometries evince that a twist of 90° of $N(CH_3)_2$ produces minimum energy state and maximum dipole moment change. The experimentally measured value (9.23 D) for dipole moment change from ground to excited state tallies with the corresponding value computed theoretically (7.5 D) for twisted geometry. Polarization studies in polar, nonpolar solvents and in β-CD cavity suggest that the emission transition moment is perpendicular to the molecular axis confirming the presence of twisted conformer. Weak acid protonates the carbonyl group while strong acid favors protonation of amino nitrogen. The solvent dependent absorption and emission spectra were found to be due to intramolecular structure change rather than 'solvent coordinate' effect. TICT band intensity is enhanced in β-CD inclusion complex due to modulation of photophysics by it while the normal (DE) band failed to appear. The fluorescence dependence of DMACA inclusion complex on polarity and viscosity has been discussed in detail. Quantum chemical calculations with AM1 Hamiltonian have been performed to find the actual geometry producing twisted intramolecular charge transfer state by twisting $N(CH_3)_2$ group to different angles and to confirm experimental findings qualitatively.

Keywords: 4-Dimethylamino cinnamic acid; Fluorescence; Excited-state dipole moment

1. Introduction

Photo-induced charge transfer (CT) is the most familiar reaction in photochemistry and photobiology. Molecules containing donor and acceptor groups undergo charge separation in an excited electronic state in the following way [1]

$$DA+h\nu \rightarrow (DA)^* \rightarrow D^+A^-$$

The D^+A^- state, strongly charge transfer in character, has been conceptualized to produce a twisted form in excited state, which allows for total charge separation and that is stabilized in polar environment. Dimethyl aminobenzonitrile (DMABN) is the first candidate to show anomalous spectroscopic properties, i.e., dual fluorescence [2–7] in polar environment due to adiabatic photoreaction. Lippert et al. [2] assigned the first one as benzene derivatives like normal band (B band), originated from ^1L_b type state and proposed the origin of the anomalous or long wavelength second band (A band) as a result of solvent induced reversal of excited state which is more polar ^1L_a type state. According to them the corresponding emitting states of the dual bands are B* and A*, which are controlled by thermally equilibrated rate constants K_{BA} (forward reaction) and K_{AB} (backward reaction). Rotkiewicz et al. [3] later put forward a suggestion to explain the anomalous fluorescence band partially supporting Lippert et al. that the equilibrium between B* and A* is not maintained thermally. It is rather maintained through dynamic relaxation of DMABN with internal twisting of dimethylamino group involving electron transfer from electron rich amino group to cyano or entire benzonitrile group. This suggestion was established by various steady state and time-resolved experiments although strong controversy is still there regarding this interpretation of twisted intramolecular charge transfer (TICT) states. Leinhos et al. [8], Visser and Varma [9], and Visser et al. [10] have explained, the source of anomalous fluorescence as exciplex fluorescence and solute–solvent exciplex fluorescence respectively [8–10].

* Corresponding author. Tel.: +91-33-476-4971; fax: +91-33-473-2805; e-mail: spsc@iacs.ernet.in

1010-6030/98/$ - see front matter
PII S1010-6030(98)00303-7

Also it is important to note that the quest for a satisfactory explanation is still being vigorously pursued in several laboratories. Extensive studies were done in last two decades in searching the twisted intramolecular charge separation state. The fluorescent anisotropy associated with electron transfer between two different species of a molecule separated by essential single or double bond is a phenomenon that has significant diagnostic application in many systems such as, tailor made fluorescence dyes, sensing of free volume polymers, fluorescent pH or ion indicators fluorescent solar collectors and electron transfer photochemistry [11–17]. Now the controlling of internal rotation of a fluorophore and to find one efficient fluorescing system have been a subject of considerable interest of experimental and theoretical work in recent years, because TICT often plays a typical role as a fluorescence quencher. The control of intramolecular rotation is made possible by one of the two ways: the first one is to impose the external constraint on the molecule and the second one is to destroy the flexibility of the molecule. 4-Dimethylamino cinnamic acid (DMACA) may be a likely candidate for making TICT-like state model in which the amino group may transfer an electron to the carbonyl group or better to the π_z^* orbital extending over the entire cinnamic acid group.

β cyclodextrin (CD) contains seven units of glucose of toroidal hollow shape whose internal diameter is approximately 7 Å. The spatial arrangements of functional groups in CD.X molecules result in a variety of interesting features of these compounds. The exterior part of the β-CD is hydrophilic and the interior is relatively hydrophobic. β-CD has a property to form supramolecular structure providing relatively nonpolar micro-vessel environment to the guest molecule through the non-covalent interaction [18] and the guest molecules are stabilized within the cavity of the β-CD primarily by hydrophobic forces. The supramolecular structure, especially the inclusion complex may have different photophysical properties. In 1:1 inclusion complex the host molecules provide single micro-vessel to a guest molecule, which may impose certain degree of constraint to the guest. So we can expect the intramolecular phenomena from the guest molecule of 1:1 host–guest inclusion complex. In this paper it is thought to unravel some questions regarding the photophysical properties of DMACA due to the introduction of CH=CH chain between phenyl ring and carbonyl group and also to interpret the modulation of photophysics due to DMACA:β-CD complexation in the light of possible TICT concept or a possible umbrella motion of amino group.

2. Experimental

DMACA was synthesized by the well-known Reformatsky reaction. In short, ethyl bromoacetate in benzene–ether mixture was refluxed in presence of Zn-wool which on dehydration with P-TsOH in benzene altered to corresponding β ester. This ester was added with a stirred solution of sodium ethoxide in ethanol at room temperature. On completion of reaction, the mixture was acidified with dilute HCl and the separated solid was then filtered and washed in pure water. Finally purification was done by repeated crystallization. The melting point of it was verified with literature before use.

The solvents ethanol (EtOH), methanol (MeOH), acetonitrile (ACN), 1-butanol (BuOH), *N*,*N*-dimethyl formamide (DMF), acetone (ATN), tetrahydrofuran (THF), diethylether (DEE), dichloroethane (DClE), acetic acid and hydrochloric acid (HCl) (E. Merck, spectroscopic grade) were used as supplied, but only after checking the purity fluorometrically in the wavelength region of interest. The solvent, methyl cyclohexane (MCH) (Spectrocheme, India) was distilled in vacuum and tested for the absence of any emission in the wavelength regions studied.

Absorption and emission spectra were recorded on a Shimadzu UV–VIS scanning spectrophotometer model UVPC 2101 and Hitachi spectrophotometer model F-4500, respectively. Spectrum correction has been performed to enable measuring a true spectrum by eliminating instrumental response such as wavelength characteristics of the monochromators or detectors. For all measurements, the sample concentration was restricted at $\sim 10^{-5}$ M in order to avoid aggregation problem, self quenching etc. The phosphorescence lifetime was measured from the decay of phosphorescence intensity with time. The relative quantum yields were measured from corrected area under the emission curve according to the equation [19,20] taking 9,10-diphenyl anthracene as standard ($\varphi = 1$). The ground state dipole moment (μ_g) of the molecule has been measured in acetonitrile solution using relation [19,20]

$$\mu_g^2 = 9KT(\varepsilon_s - \varepsilon_\infty)(2\varepsilon_s + \varepsilon_\infty)/[4\pi N_1 \varepsilon_s (\varepsilon_\infty + 2)^2].$$

where N_1 = number of solute molecules per cubic centimeter of the solution, K = Boltzmann's constant, T = absolute temperature, ε_s = static dielectric constant of the solution measured as the ratio of capacitance of the solution to the capacitance to the air, and ε_∞ = infinite frequency dielectric constant nearly equal to η^2 (η = the refractive index). The refractive index and static dielectric constant were measured by Abbe refractometer and Impedance Analyzer model HP 4192A, respectively.

The degree of polarization of fluorescence at different temperatures and degree of phosphorescence polarization was obtained by using a modified polarizer accessory with the Hitachi F-4500 spectrophotometer. The degree of polarization P is defined as [19,20]

$$P = \frac{I_\parallel - GI_\perp}{I_\parallel + GI_\perp}$$

where $I_\parallel$ and $I_\perp$ are the intensities of the emitting light polarized with electric wave vector perpendicular and parallel respectively to the exciting light, which is polarized with electric vector perpendicular to the plane containing the exciting and emitting beam. G is a polarization correction factor of the fluorescence spectrophotometer.

The time resolved fluorescence decay of PBA in ACN was observed by employing a CW mode-locked frequency doubled Nd-YAG laser-driven dye (Rhodamine 6G) laser operating at a repetition rate of 800 kHz with pulse width of the order of 4–10 ps [21]. Fluorescence lifetime in ACN was obtained by using a time-correlated single-photon-counting coupled to a micro channel plate photomultiplier (Model 28090; Hamamatsu). The instrument response function (IRF) was obtained at 295 nm using a dilute colloidal suspension of dried nondairy coffee whitener. The cut-off filter was used to prevent scattering of excitation beam and the emission was monitored at the magic angle (54.7°) to eliminate the contribution from the decay of anisotropy. The fluorescence lifetime in MCH was measured by using single-photon-counting fluorimeter (Edinburgh Instrument, UK) with excitation source N_2-filled nanosecond flash lamp.

For the luminescence study in cyclodextrin cavity, β-CD was used as received from Aldrich Chemical, USA. The sample concentration of the solution was maintained to keep constant (10^{-5} M) for all different β-CD concentrations. The stock solution of β-CD was made with water deionized by a MilliQ plus water purification system (Millipore, USA) and desired dilution was made from stock solution. Isosbestic points were used to excite the molecule and to calculate dissociation constant.

3. Results and discussion

3.1. Absorption spectra

DMACA shows a strong structureless broad absorption spectra whose λ_{max} lies in the range of 320 nm to 363 nm (Fig. 1). This spectrum has two peaks. The weak higher energy 320 nm band is partially hidden under the envelop of the strong long wavelength 364 nm band. Comparing the position and molar absorption coefficient with benzene derivatives, we can assign these bands as ^1L_b and ^1L_a, respectively [22]. The long wavelength 364 nm band shifts towards the blue region according to the strength of the hydrogen bonding property of the solvent (Table 1). The extent of shift is such that the first band nearly overlaps the second band producing single peak absorption band of DMACA in Millipore water. In non hydrogen bonding solvent, i.e., in aprotic solvent (polar), the 364 nm band shows large red shift on solvent polarity while the higher energy band remains unaltered. The strong hypsochromic shift of the first band by hydrogen bonding solvent may indicate the possibility of hydrogen bonding between solvent and DMACA in the following manner (Scheme 1).

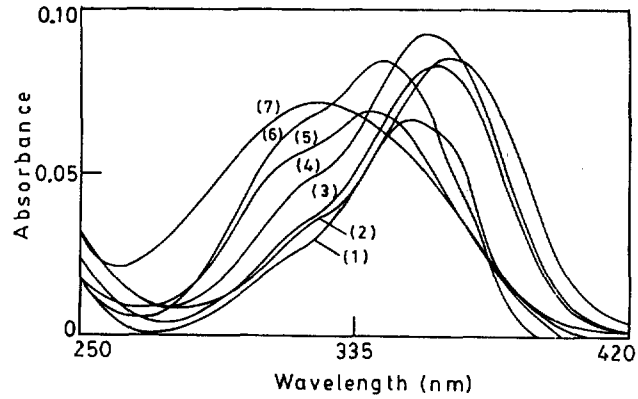

Fig. 1. Electronic absorption spectra of DMACA in the concentration range of 10^{-5} M at 300 K in a 1 cm cell in different solvents. (1) MCH, (2) $CHCl_3$, (3) ACN, (4) *N,N*-DMF, (5) EtOH, (6) MeOH, (7) water.

The property, that DMACA is weakly soluble in nonpolar solvents and strongly soluble in polar solvents is indicative of DMACA being polar in ground state. Now from the aprotic

Table 1
Absorption fluorescence data of DMACA at 300 K

Solvent	Absorption data			Fluorescence data				
				DE		TICT		φ
	ε ($\times 10^{-3}$ M)	λ_{max} (nm)	ν_{max} ($\times 10^{-3}$ cm^{-1})	λ_{max} (nm)	ν_{max} ($\times 10^{-3}$ cm^{-1})	λ_{max} (nm)	ν_{max} ($\times 10^{-3}$ cm^{-1})	
MCH	–	352	28.4	391	25.57	–	–	0.07
n-Heptane	–	353	28.3	391	25.57	–	–	0.065
ATN	7.1	362	27.62	391	25.57	440	22.7	0.018
DCIE	6.19	364	27.47	391	25.57	437	22.88	0.02
THF	5.8	363	27.55	391	25.57	435	22.98	0.026
DEE	5.6	361	27.7	392	25.61	425	23.53	0.03
ACN	8.3	363	27.55	391	25.57	460	21.74	0.04
$CHCl_3$	5.75	364	27.4	391	25.57	438	22.83	0.026
EtOH	5.78	340	29.4	391	25.57	441	22.67	0.014
MeOH	5.5	344	29.0	391	25.57	442	22.62	0.016
N,N-DMF	5.67	360	27.7	391	25.57	445	22.47	0.03
H_2O	6.89	323	30.9	–	–	466	21.59	0.03
H_2O + β-CD	7.5	335	29.85	–	–	450	22.22	–

M = dm^3 mol^{-1} cm^{-1}.

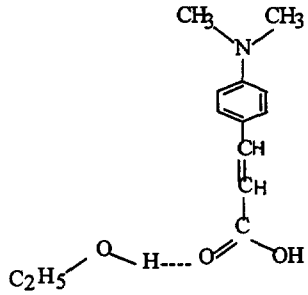

Scheme 1. Hydrogen bond formation of DMACA in ethanol.

solvent effect we tentatively assign the first band as charge transfer (CT) band. Besides, in aqueous solution addition of a little amount of 0.1 N HCl vanishes both the bands and produces a new band at 268 nm but in very weak acid solution (0.1 N CH_3COOH) the absorption spectra was found to be largely red shifted producing absorption λ_{max} in the region of 360 nm. On the other hand, addition of same amount of 0.1 N NaOH makes no change of absorption band system. Two possibilities could be proposed for this typical behavior of DMACA in acidic solution. Firstly, due to addition reaction of α, β unsaturated carbon and HCl and also due to protonation, the necessary conjugation of the molecule breaks down leaving off the absorption spectrum. In this case phenyl ring acts as a fluorophore of that new species, which shows the new absorption band system with a new band at 268 nm. Secondly, DMACA has resonance structures 'a' and 'b' in water solution and the red shift of absorption band in weak acid due to the protonation of carbonyl group in structure 'c' (Scheme 2). But in moderate to strong acid solution the amino group gets protonated (Scheme 2) like other amino acid glycine and histidine [23] which in turn breaks the conjugation of the system, and hence there is no absorption band in 320–360 nm region. The 268 nm absorption band in strong acid solution appears due to the phenyl ring. In a very closely related molecule 4-dimethyl aminobenzoic acid, two pK_a values one at 6 and other at 11 [24] could be found due to protonation of amino and benzoic acid groups respectively and in DMACA the pK_a values would be very similar to this.

3.2. Emission spectra at 300 K

DMACA in different polar solvents exhibits dual fluorescence (Fig. 2) consisting of two distinctive bands, the structureless anomalous long wavelength A band at about (420–466) nm and short wavelength B band at (391–393) nm wavelength region, Table 1. In non polar hydrocarbon solvents it shows only one fluorescence band with increased quantum yield, nearly at the same position of B band that has been assigned in the case of polar solvent. The origin of B band is assigned as benzene $^1B_{2u} \rightarrow {}^1A_{1g}$ transition, which is a delocalized excited state in phenyl ring [25,26] (DE). The position of B band remains nearly unaffected by solvent polarity but the anomalous A band shows a large red shift from polar to more polar solvents with decreasing quantum

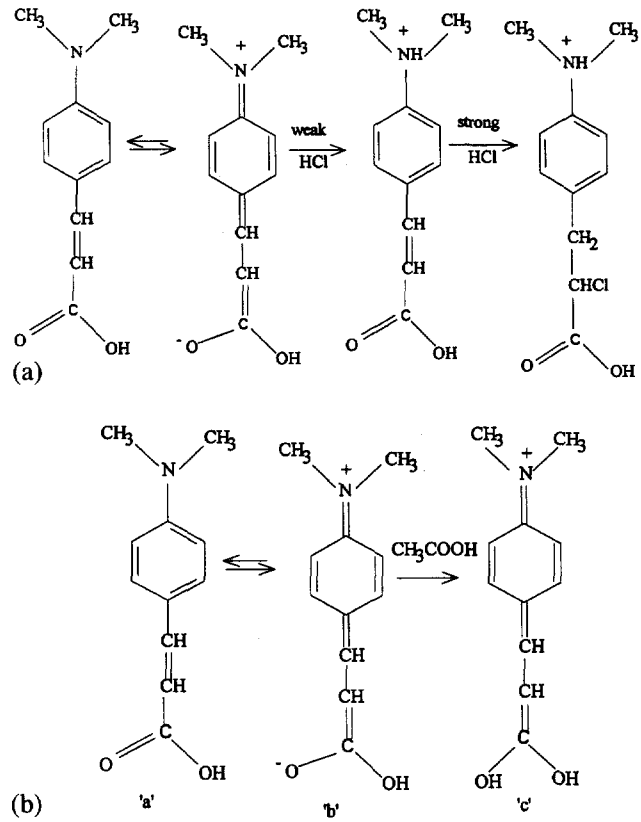

Scheme 2. (a) Protonation of DMACA by strong acid. (b) Resonance structure and protonation of DMACA by weak acid.

yield (Table 1). The intensity of B band in polar solvent is very low and in extreme case the presence of B band is hardly observed. In that case the B band goes underneath the envelop of the A band fluorescence. The fluorescence intensity and fluorescence peak positions of dual fluorescence are independent of excitation wavelength over the large range of absorption band. Also the fluorescence intensity is nearly

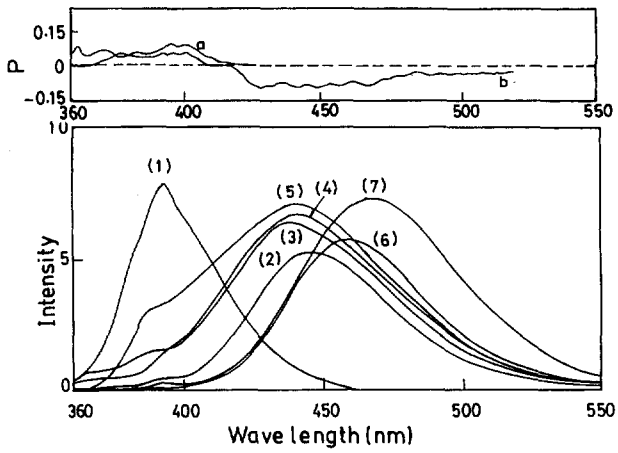

Fig. 2. Corrected fluorescence emission and fluorescence emission polarization spectra of DMACA at room temperature ($c \sim 10^{-5}$ M) in different solvents. (1) MCH, (2) *N,N*-DMF, (3) $CHCl_3$, (4) MeOH, (5) EtOH, (6) ACN, (7) water and (a) fluorescence emission polarization spectra of DMACA in MCH and (b) fluorescence emission polarization spectra of DMACA in EtOH. ($\lambda_{exc} = 350$ nm).

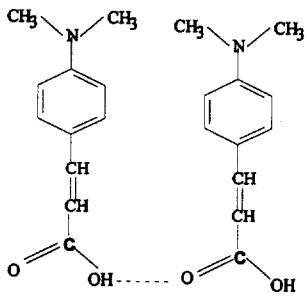

Scheme 3. Dimer formation through H-bonding.

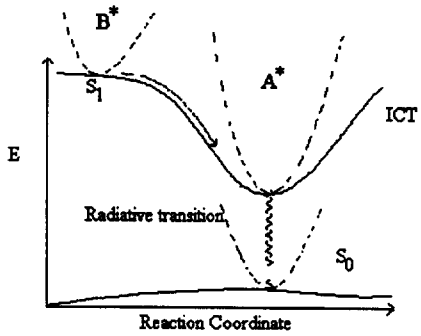

Scheme 4. Energetically favorable internal process.

independent in the concentration range (10^{-5}–10^{-6}) M. The intensities of both bands decrease with increasing concentration and at concentration of 5×10^{-3} M the fluorescence nearly vanishes. This finding points that at higher concentration DMACA form dimer by H-bonding between acid parts of two molecules (Scheme 3). To avoid the formation of dimeric form, all fluorescence studies have been confined to the sample concentration less than 10^{-5} M.

It may be concluded regarding the decrease of B band and appearance of A band in polar solvent of DMACA that a reaction path exists in the excited state leading from the delocalized state (emitter of B band) to a photochemical product with energetic minimum forming an ICT state (emitter of A band). These two emitters are called B* and A* states, which have been shown in Scheme 4. These photochemical paths later substantiated by the surface crossing of ^{1}B and ^{1}A states in quantum chemical calculations (Section 5).

The large red shift of A band with respect to polarity effect of the solvents may be rationalized by the dipole moment change of DMACA from ground state to excited state [27]. From solubility properties and absorption spectra we may guess the molecule may have ground state dipole moment, which has been measured to be 3.89 D. Again from quantum chemical calculation we get the ground state dipole moment to be 4.04 D. Now, taking account solvatochromic shift and using Lippert–Mataga relation [28], the computed ($\mu_e-\mu_g$) or $\Delta\mu$ is 9.23 D. The quantum chemical calculation also predicts large dipole moment change = 7.5 D. This large dipole moment change in excited state, suggest that there has been redistribution of charge in excited state, which then causes the possibility of making ICT state or TICT state. In the case of DMACA the $N(CH_3)_2$ group is linked to the phenyl ring by essential single bond and if it favors the twisting of $N(CH_3)_2$ in excited state then the resulting full charge transfer may possibly cause a TICT state. It is also important to note here that the measurement of B band fluorescence quantum yield in polar solvent is impossible due to low intensity. The quantum yield of A band fluorescence has been measured in different polar protic and aprotic solvents and this yield has a linear dependence with polarity. With decrease of polarity for the aprotic solvents, the quantum yield of A band fluorescence increases. In more polar solvent the A* state is more stabilized by solvation, which decreases the energy gap between ground state and A* state resulting the enhancement of nonradiative transition from A* to S_0.

In acidic medium DMACA shows no trace of fluorescence. This is probably due to protonation of DMACA, which decreases the donating property of amino group resulting no emission, but in basic solution no change in emission properties could be observed.

3.3. Emission in solvent mixture

To study the role of solvent molecules in the intramolecular CT process of excited DMACA molecule and hopefully to gain a better understanding of the coupling between the twisting motion and solvent relaxation, the fluorescence properties of DMACA in mixed solvents were investigated. The basic thing is to control the local number density of the polar solvent molecules without greatly altering the viscosity of the solution and it may provide the information about the effect of the change in local dipole density on the dynamics and yield of the CT process.

We have chosen to study the mixed solvent system ethanol and MCH because of their nearly similar viscosity. In hydrocarbon solvent the DMACA shows only one band that has been assigned as normal band of DE state [25,26] but addition of ethanol in hydrocarbon solvent enhances the second band keeping the first band unaltered. The Fig. 3 shows successive enhancement of A band with addition of ethanol and 10% ethanol mixture of MCH solution produces nearly same fluorescence spectra as pure ethanol solution. This observation evinces that the addition of ethanol in MCH solution increases the micro polarity of the medium which then sta-

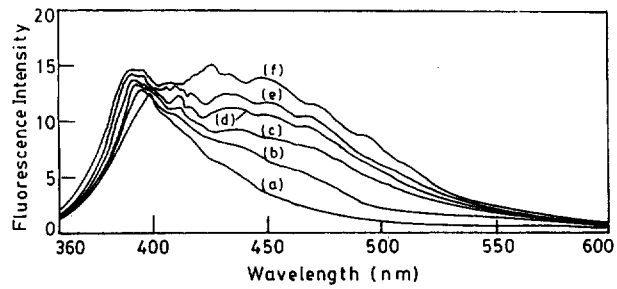

Fig. 3. Corrected fluorescence emission spectra of DMACA in MCH and EtOH mixture. (a) MCH, (b) MCH + 2% EtOH, (c) MCH + 4% EtOH, (d) MCH + 6% EtOH, (e) MCH + 8% EtOH, (f) MCH + 10% EtOH. (λ_{exc} = 350 nm).

bilizes the transition state for a TICT process, if any. This stabilization goes away after removal of ethanol from the mixture by slow evaporation and the original single band B fluorescence spectra appeared like pure MCH solution. The same type of result was observed when traces of water present in MCH solvent.

3.4. Viscosity effect on emission

To ascertain the nature of ICT band the emissions were studied in media of increasing viscosity a well-established technique. Fig. 4 shows the fluorescence spectra of DMACA in glycerol and methanol mixture, as a function of glycerol concentration. DMACA fluorescence spectrum in mixture is nearly identical type of spectrum produced in methanol. Enhancement of fluorescence quantum yield of second band (A) and a bathochromic shift of 1082 cm^{-1} could be observed as we go from pure methanol to 95% glycerol. The reverse process, i.e., decreasing viscosity of mixture by successive addition of methanol produces the nearly same fluorescence intensity as in methanol. Of the two said effects, bathochromic shift of DMACA could easily be explained from polarity point of view of the solution. Glycerol, being more polar than methanol, stabilizes the charge transfer state to a greater extent and hence the red shift. Fluorescence enhancement (or hyperchromic effect) could well be explained from macroviscosity point of view. Here the twist of $N(CH_3)_2$ around C–N bond, if any, would greatly be hindered in viscous glycerol. In absence of such twist, possibly the 'umbrella motion' of dimethylamino group [29] ushers in charge transfer from donor to acceptor moiety and the overlapping of donor and acceptor π-orbitals is maximum. Greater mixing of DE and charge transfer states thus leads to strong transition moment and radiative transition. Here the results show that the ICT state is affected by macroviscosity which is the general trend [30,31] though the contrary result [32,33] found for the dimethylamino benzonitrile in β-CD cavity.

3.5. Emission at 77 K (glass matrices)

In a similar note of the viscosity effect (vide supra) an emission study has also been made in glass matrix to determine the nature of ICT state. At low temperature (77 K) both in hydrocarbon glass and ethanol glass DMACA show well resolved (Fig. 5) single band (only B band). In nonpolar hydrocarbon glass a blue shift (130 cm^{-1}) was observed in fluorescence spectra with respect to ethanol glass. Normally in glass matrices all probable photoreaction ceases resulting in increase in normal fluorescence. In MCH glass, the fluorescence quantum yield increases to nearly 7 times (Table 2) to that at room temperature but in ethanol glass the increment is more or less 50 times than the yield at room temperature. This abrupt relative increase of quantum yield may be

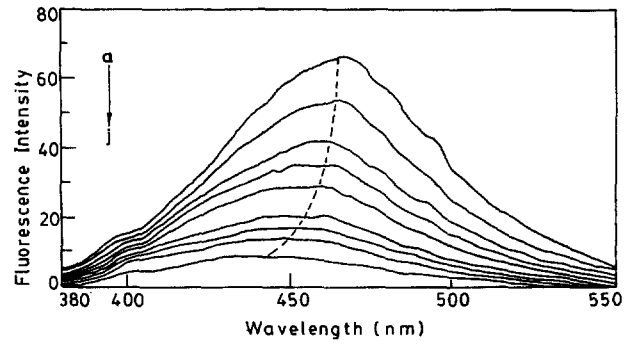

Fig. 4. Corrected fluorescence emission spectra of DMACA in glycerol and methanol mixture. Viscosity dependence emission spectra of DMACA in room temperature. (a) 95% glycerol, (b) 85% glycerol, (c) 73% glycerol, (d) 60% glycerol, (e) 48% glycerol, (f) 37% glycerol, (g) 30% glycerol, (h) 23% glycerol, (I) pure methanol. (λ_{exc} = 350 nm).

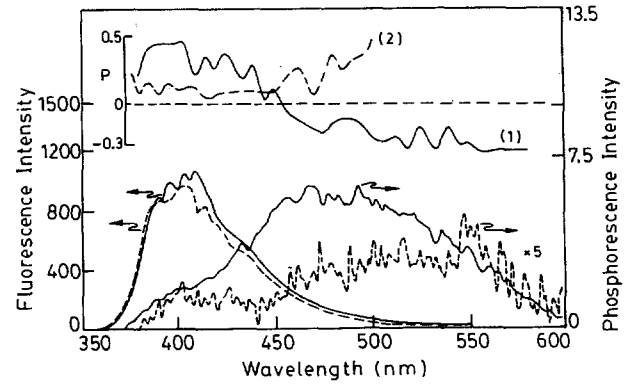

Fig. 5. Corrected fluorescence, phosphorescence and fluorescence phosphorescence polarization spectra in (- - -) MCH and (———) EtOH glass at 77 K, respectively.

Table 2
Fluorescence and phosphorescence data of DMACA at 77 K

Solvent	Fluorescence data			Phosphorescence data			
	λ_{max} (nm)	ν_{max} ($\times 10^{-3}$ cm^{-1})	φ_{fl}	λ_{max} (nm)	ν_{max} ($\times 10^{-3}$ cm^{-1})	φ_P	τ_P (s)
MCH	400 (3.1 eV)	25.00	0.7	400 (3.1 eV)	25.0		0.149
				464 (2.67 eV)	21.55		0.129
				500 (2.48 eV)	20.0	0.005	0.124
				550 (2.25 eV)	18.18		0.119
EtOH	400 (3.1 eV)	25.00	0.78	400 (3.1 eV)	25.0	0.025	0.26
				464 (2.67 eV)	21.55		0.19

rationalized as rigid glass matrices (77 K) provide no room for twisting motion of $N(CH_3)_2$ group in excited state and the TICT emission (A band) does not appear at 77 K glass thereupon. Incidentally, the TICT state is the main non-radiative channel of room temperature fluorescence resulting a decrease in quantum yield in a drastic way. DMACA also shows phosphorescence (Fig. 5) in ethanol and MCH glass matrices along with high fluorescence quantum yield. The phosphorescence spectra of DMACA composed of two distinctive bands in ethanol glass around 400 nm and 465 nm. The phosphorescence spectrum is more structured in MCH glass than in ethanol glass, although it is too weak to study. In ethanol the lifetime of phosphorescence at 400 nm is 11 ms and at 465 nm is 26 ms. These two distinctively different lifetimes indicate that these bands arise from two different excited triplet states [34]. On the basis of two lifetime data a clear cut assignment of (n,π*) or (π,π*) triplet state might not be possible. On the other hand, in MCH glass phosphorescence lifetime shows nearly constant value of 13 ms throughout the phosphorescence spectrum. This interesting result indicates that a possible vibrational coupling might exist between two excited triplet states, which is strong in MCH glass. A polarization study of phosphorescence spectra may give some insight to this (vide infra).

3.6. Polarization spectra at room temperature and at 77 K

Fig. 2 depicts the fluorescence polarization spectra of DMACA in MCH and ethanol solvents at room temperature. In MCH solvent the degree of fluorescence polarization P is positive throughout the fluorescence band. So this negates the possibility of having other hidden band under the envelope of the normal B band fluorescence. But in ethanol solvent the degree of fluorescence polarization is positive at 390 nm region and negative at 440 nm region. This change of P values from positive to negative in polar medium indicates the presence of two bands (in this case B and A band) with transition moments mutually perpendicular direction [35]. In MCH solvent absence of A band is corroborated by zero value of P at long wavelength region (Fig. 2). The positive value of P in B band region indicates that the nonpolar (NP) emission (i.e., DE state emission) is polarized along molecular long axis, i.e., the first excited singlet state has an in-plane molecular long axis polarization. One might argue that the polarization study in solvent media is affected by rotational depolarization. This possibility may be ruled out because the fluorescence polarization spectrum of DMACA in highly viscous glycol media shows the same as in Fig. 4. Besides this, the rotational relaxation time of DMACA computed from Smoluchowski–Einstein relation $\rho = 3\eta v/RT$ [35] to be 2.3 ns that is large enough compared to the fluorescence lifetime of B band (Table 3). Again the nearly large constant negative value in A band region evinces that the A band emission is polarized perpendicular to the molecular long axis. In other words the A band emission originates from orthogonal intramolecular charge transfer state that is only possible by the twist of $N(CH_3)_2$ group in excited state as the rotation of acid group makes no change (vide infra). Turning back to the discussion of the emission from glass matrices (vide supra), we find that the polarization results also corroborate the assignment of A and B bands. Both in ethanol and in MCH glass the fluorescence polarization has positive P value throughout the whole fluorescence band (Fig. 5). This P value confirms that, both in polar and nonpolar matrices DMACA has no excited state responsible for A band emission also it indicates that the B band is polarized along the molecular long axis. In ethanol glass the phosphorescence polarization (Fig. 5) was found to vary from positive to negative value. It is interesting to note that the phosphorescence band appearing at fluorescence B band region has a positive P value and the phosphorescence band appearing at fluorescence A band (at room temperature) has a negative value. These positive and negative P values clearly establish that, at least two excited triplet states are present in DMACA, which have mutually perpendicular transition moments responsible for phosphorescence spectra. Moreover, the variation of P with wavelength in the phosphorescence spectrum is quite indicative of a possible vibronic coupling between the triplet states [19,20] as indicated in Section 3.5.

Table 3
Excited state depletion rate parameters of DMACA at 300 K

Solvent	Total φ_{fl}	τ_{fl} (ns)	K_r ($\times 10^{-8}\,s^{-1}$)	K_{nr} ($\times 10^{-8}\,s^{-1}$)
MCH	*0.7*	*0.75*	*9.3*	*4.01*
ACN	*0.04*	*0.11*	*3.7*	*87.3*
ACN	0.04	0.109	3.65	88.1
$CHCl_3$	0.026	0.1	2.5	97.4
EtOH	0.014	0.06	2.5	164.5
MeOH	0.016	0.07	2.4	140.6
N,N-DMF	0.03	0.12	2.5	80.8
H_2O	0.03	0.1	3.0	97.0

Values in italic font indicate the measured value.

3.7. Kinetic aspect of ICT

The fluorescence decay of DMACA at B band in MCH is mono exponential with decay time 750 ps and the same in ACN is 150 ps. Obviously, these two lifetime values confirm the lower quantum yield as well as lower intensity B band of DMACA in acetonitrile than methylcyclohexane. So in acetonitrile B* state is more favorably deexcited through nonradiative path within the lifetime of B* state. Now the mono exponential fluorescence decay of A* band in ACN has a lifetime of 110 ps that is close to that of B* band. As we do not see the rise time of A* band it is possible that the rise time is too fast to be able to detect under the present condition. Some charge transfer process was found to occur within a time constant of 10 ps [36]. This rise time of A* band is the sum of forward and backward equilibration rate between DE and ICT (or TICT) states [37] as predicted from kinetic analysis. Scheme 4 postulates the relation between B* and

A* states. It is more important to note here that, DE band intensity decreases concomitantly with the increase of ICT band in polar solvent that might reflect that the formation of ICT state is out of DE state, i.e., there might be some parent daughter relationship between the two states.

The excited state lifetime and non-radiative rate K_{nr} constant of DMACA in different other solvents have been computed in the following way [38].

$$\tau_{fl}=\varphi_{fl}/K_r \quad (1)$$

and

$$K_{nr}=(1-\varphi_{fl})/\tau_{fl} \quad (2)$$

where $K_r=4.4\times10^4$, ε_a and φ_{fl} is the total fluorescence quantum yield of DMACA in different polar solvents. Again the radiative and non radiative rate constants of DMACA have also been computed in MCH and ACN using the measured fluorescence lifetime and fluorescence quantum yield. Since, the DE band is too weak to measure the quantum yield, we assume that the total quantum yield is mainly responsible for ICT emission only in polar solvent. So roughly, the calculated lifetime is an indicative of ICT fluorescence lifetime (Table 3).

Phosphorescence quantum yield of DMACA is very low (discussed in Section 3.6), which indicates the probability of intersystem crossing is not the main non-radiative path of DMACA, rather the non-radiative deactivation of this molecule is mainly due to internal conversion. Table 3 shows that the rate constant of non-radiative process is very high and always greater than the radiative rate constant. The internal rotation, i.e., twisting of $N(Me)_2$ group of the molecule is one of the possibilities of internal conversion other being umbrella-like mode of amine. In view of the conclusion from polarization spectra favoring rotation of $N(Me)_2$ group we believe that the last possibility does not contribute much to the charge transfer state in ethanol. Planar ICT state, which is ascribed by the statistical weight of resonance structure 'a' in Scheme 2, also explains the solvent polarity effect. Since TICT state is main non-radiative process in ICT state, which automatically decreases the quantum yield and lifetime of the normal fluorescence. The fluorescence lifetime is too low to promote ICT state without twisting. In Section 4 emission and absorption studies on DMACA encapsulated in cyclodextrin cavity will corroborate the findings here about TICT and the related photophysics.

4. Luminescence and absorption of supramolecular complex between β-CD and DMACA

4.1. Absorption spectra

In order to characterize the nature of charge transfer state and to have a better understanding of photophysics, the emission and absorption studies of DMACA in β-CD cavities have been done. Fig. 6 shows the absorption spectra of

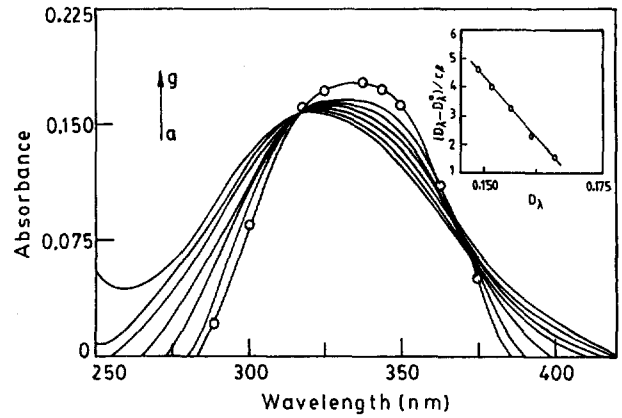

Fig. 6. Electronic absorption spectra of DMACA as a function of β-CD concentration in aqueous solution. (a) 0, (b) 8.125×10^{-4} M, (c) 1.625×10^{-3} M, (d) 3.25×10^{-3} M, (e) 6.5×10^{-3} M, (f) 1.3×10^{-2} M, and (g) calculated absorption curve for infinite concentration of β-CD. Inset is the plot of $(D_\lambda-D_\lambda^0)/C_\beta$ against D_λ where $\lambda_{exc}=350$ nm.

DMACA as a function of β-CD concentration. With increase of concentration of β-CD, the absorption maximum for neat DMACA is shifted with slight increase of molar absorption coefficient. Two distinct isosbestic points are observed at 320 nm and 364 nm, respectively, which confirms the involvement of one-to-one complexation between fluorophore and β-CD [30–32] and the equilibrium may be described as

$$DMACA+\beta\text{-}CD\leftrightarrow DMACA\cdot\beta\text{-}CD$$

The equilibrium constant K ([DMACA·β-CD]/[DMACA]·[β-CD]) has been calculated from Eq. (3).

$$(D_\lambda-D_\lambda^0)/C_\beta=K(D_\lambda^\infty-D_\lambda) \quad (3)$$

where C_β is the concentration of the β-CD and D_λ, D_λ^0 and D_λ^∞ are absorption coefficient at a wavelength of λ at a particular concentration C, in the absence of β-CD and at infinite concentration of β-CD, respectively. The values of K and D were calculated from the slope and intercept of the plot $(D_\lambda-D_\lambda^0)/C_\beta$ vs. D_λ (Fig. 6). K was calculated to be 184 ± 10 at 300 K. Using the Eq. (3), D_λ^∞ is calculated for different λ and a plot of D_λ^∞ against λ has been shown in Fig. 6. The peak of the calculated absorption spectra of inclusion complex reaches at 354 nm. It is observed from the Fig. 6 that the steepness of the absorption curve increases when molecules go from water to β-CD cavity. With the increase of β-CD concentration this steepness also increases. The steepness of absorption band, as well as the red shift of absorption λ_{max} indicate different type of interaction in cyclodextrin cavity compared to pure water [35]. From solvent dependent absorption spectra of DMACA we observe a hydrogen bonding interaction in different aprotic solvents (Section 3.1) involving the terminal carbonyl group lone pair [35] where the solvents act as hydrogen bond donor. In water this propensity was found to increase many more times as confirmed by blue shift of absorption λ_{max} (i.e., reduction of conjugation) compared to ethanol and methanol solvent. But in the case of β-CD inclusion complex, the guest molecule is

encapsulated by the cavity of host molecule providing less polar micro environment, which may obstruct the forming of hydrogen bond with other molecules and hence the red shift and steepness of absorption in β-CD solution.

4.2. Emission spectra

In aqueous solution DMACA shows negligible amount of B band emission and a prominent TICT emission. Fig. 7 shows the emission spectra of a series of DMACA solutions at different β-CD concentrations when excited by 320 nm, one of the isosbestic points in absorption spectra. No distinct appearance of B band could be detected with β-CD complexation, although β-CD inclusion complex provides a nonpolar environment to the guest molecule [39] while in neat nonpolar media DMACA shows prominent B band. This contradictory result suggests that β-CD cavity environment may not be pure nonpolar to produce B band emission of DMACA. On the other hand, A band emission of DMACA was found to increase with increasing concentration of β-CD along with sufficient blue shift. It is also important to note that the same type of emission with decreased intensity could be observed when DMACA is excited by the other isosbestic point (374 nm) of absorption spectra (Fig. 6).

The degree of polarization of A band emission in β-CD inclusion complex is less than that in water solution (Fig. 7). In both the cases the degree of polarization is negative, which indicates that the A band emission is polarized perpendicular to the molecular long axis [36]. The reduction in magnitude of degree of polarization in β-CD complex would suggest that, the perpendicularity of TICT emission polarization might be destroyed to some extent due to less amount of rotation of $N(CH_3)_2$ in β-CD cavity. The excitation spectra of DMACA in water solution and in β-CD inclusion complex in slightly different from the absorption spectra. The two isosbestic points shift towards blue in excitation spectra. The first isosbestic point in excitation spectrum is at 289 nm (in absorption spectrum it is at 320 nm) and second is at 345 nm (in absorption spectrum it is at 374 nm). This difference in excitation and absorption spectra might be due to the heterogeneity in excited state solvation [40] and homogeneity in the ground state conformation.

The interior of β-CD cavity constitutes an isolated environment. The restricted shape and size of the cavity geometrically constrain the guest molecule and thereby stabilize the conformations that are less favored in free solution [41,42]. The hydrophobic nature of the cavity can affect the photo processes that are sensitive to solvent polarity. A 1:1 complex occurs only when single molecule is within the cavity. Hence the photochemistry and photophysics are restricted to the intramolecular events, which strictly confirms the population of TICT excited state of DMACA rather than the exciplex or excimer formation. The aforesaid results of DMACA in β-CD inclusion complex may be rationalized by the following possibilities. Firstly, the red shift of absorption λ_{max} and steepness of the absorption spectra may be due to breakdown

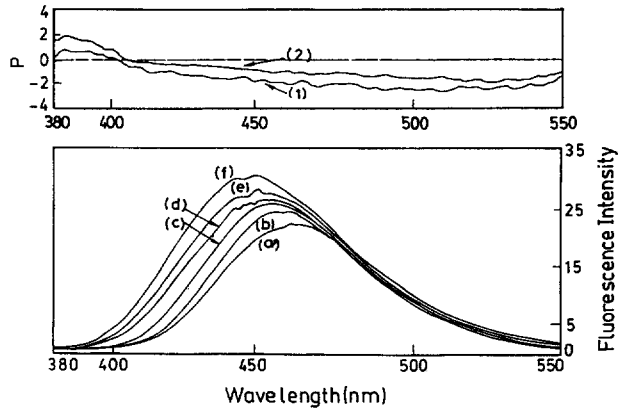

Fig. 7. Corrected fluorescence emission spectra of DMACA (3.22×10^{-5} M) in aqueous solution containing varying concentration of β-CD at 300 K. (a) 0, (b) 8.125×10^{-4} M, (c) 1.625×10^{-3} M, (d) 3.25×10^{-3} M, (e) 6.5×10^{-3} M, (f) 1.3×10^{-2} M. (1) and (2) are the fluorescence polarization spectra of DMACA in absence of ($c=1.3\times10^{-2}$) β-CD and presence of β-CD respectively. ($\lambda_{exc}=368$ nm isosbestic point).

of hydrogen bonding due to the segregation of guest molecule from water or any other molecules inside the cavity. Secondly, the blue shift of the fluorescence A band may occur probably for two reasons. When a guest molecule forms inclusion complex then its stokes loss decreases [39] which shows blue shift of the fluorescence. The β-CD cavity provides less polar environment in which the TICT state is not sufficiently stabilized by solvation [40–43], which increases the energy gap between the TICT state and ground state or low lying triplet state, resulting a blue shift. Another well-documented factor is that the bulk viscosity affects the TICT process when excited state equilibrium between DE and TICT states occurs at a time scale slower than TICT emission [42]. In bulk viscous medium (ethylene glycol), TICT emission of DMACA shows blue shift like β-CD inclusion complex. This result suggests that the orientation of the TICT fluorophore in cyclodextrin cavity may exert an influence on the TICT behavior like bulk viscous media. Hence in this case it is established that the viscosity effect of the TICT process in the cyclodextrin inclusion complex is due to slower time scale of twisting of $N(CH_3)_2$ group or solvation time [42,44]. Thirdly, the enhancement of fluorescence spectra of DMACA due to inclusion in the β-CD cavity is ascribed to the elimination of water molecules surrounding the fluorescent molecule in aqueous solution, which eliminates the nonradiative quenching channel [45] of hydrogen bond.

Again, the radiative transition of TICT state to ground state involves two orbitals located on different π-systems perpendicular to each other. Generally, it is overlap forbidden and thus expected to possess a small transition moment [42]. Due to geometrical constraint of the cavity, the involved two separate π-systems for TICT state may not go to the proper perpendicular position to each other, which then decreases the amount of overlap forbiddenness and increases the transition probability. Further we can propose that the less polar micro environment of β-CD cavity unable to stabilize the TICT state sufficiently by solvation [41], which goes in favor

of increasing the energy gap between TICT state and low lying triplet or ground state. This result decreases the non-radiative rate constant from TICT state. Thus the supramolecular complex of DMACA and β-CD increases the TICT fluorescence on different counts.

From the foregoing we may now explain the decrease in the degree of polarization (P) in β-CD cavity. Normally, the enhancement of TICT fluorescence is related to the less perpendicularity of two engaged π-systems and more negative value of P indicates the more polarized emission perpendicular to molecular long axis and vice versa. Hence less negative P value in β-CD cavity is indicative of less perpendicularity of polarized emission and this may be possible by less rotation of $N(CH_3)_2$ group of the DMACA due to geometrical constraint of β-CD cavity.

5. Quantum chemical calculations

In order to have a better understanding of different excited state properties and to predict nature and mechanism of charge transfer, the energies of the electronic transitions and dipole moments were calculated by MOPAC-CI (6×6) version 5 package with AM1 Hamiltonian [46–48] for DMACA in ground and excited states for planar and different perpendicular conformations. Molecular coordinates were obtained as described elsewhere [25,26]. A more precise geometry optimization was obtained by MOPAC's NLLSQ gradient minimization routine, and the energy of less than 0.12 kcal/mol was used for optimization criterion. CI calculation involves the interaction of microstates representing specific interaction of electrons in a set of molecular orbitals including highest occupied (HOMO) and lowest unoccupied (LUMO) molecular orbitals, starting with a set of electronic configuration. CI calculation also provides a possible approach to calculate both the ground and excited state energies as a function of molecular geometry.

In ground state the molecule shows nearly planar geometry, i.e., $N(CH_3)_2$ and COOH,

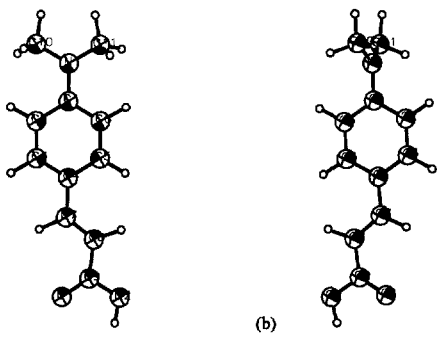

(a) Ground state optimized geometry of DMACA (b) Excited state optimized geometry of DMACA

both groups on the different planes with phenyl ring. One of the CH_3 groups takes a torsional angle 8.8° with phenyl ring and other CH_3 group has a torsional angle of 176.2° with

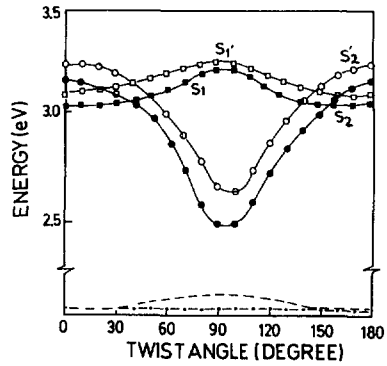

Fig. 8. Variation of ΔE ($S_1 \rightarrow S_0$), ΔE ($S_2 \rightarrow S_0$) and ground state energy with different twisted conformations. For S_1 (– ■ –) and S_2 (– ● –) when COOH in planar position and $N(CH_3)_2$ is twisted in excited state. For S_1' (– □ –) and S_2' (– ○ –) when COOH in perpendicular position and $N(CH_3)_2$ is twisted in excited state. (– ● –) and (- - -) ground state energy variation with angle of twist of COOH and $N(CH_3)_2$, respectively.

phenyl ring. The dependence of ground state energy on angle of twist of $N(CH_3)_2$ around C–N bond and COOH group around C–C bond has negligible effect, showing little rotational barrier, (Fig. 8) which confirms that the molecule favors the planar or flat conformation in ground state and also the trans isomer is more stable. On the other hand from excited state CI (6×6) calculations, we find the energy difference (ΔE) between the ^1B and ^1A (i.e., S_1 and S_2) is very low in flat geometry, i.e., in planar conformation. The energy dependence of two first excited states ^1B and ^1A on angle of twist of $N(CH_3)_2$ and COOH groups around C–N and C–C bands, respectively are shown in Fig. 8. We find that the energy maximum for the first excited singlet state (^1B) appear around 90° twisted position of $N(CH_3)_2$ group for the both situations of COOH group in planar and perpendicular positions. But the energy of ^1B state is higher when COOH group is in perpendicular position for all twisted angle of $N(CH_3)_2$ group. The variation of ^1B state energy with twist angle of COOH group around C–C bond is negligible for both positions, perpendicular and planar of $N(CH_3)_2$ group with phenyl ring. Now the energy dependence of second excited singlet state, i.e., ^1A state shows a strong minimum around 90° twisted position of $N(CH_3)_2$ group for two cases, one with COOH group in flat position and other COOH group in perpendicular position with phenyl ring. In this case no distinctive variation of ^1A state energy is permitted for twisting COOH group around C–C bond for two different positions of $N(CH_3)_2$ group, planar and perpendicular with phenyl ring. So the twist of $N(CH_3)_2$ group around C–N bond is energetically favorable for excited ^1A state. In flat geometry two states are very close for both situations of COOH group and in 30° twisting position of $N(CH_3)_2$ there is a surface crossing between the two states. These findings confirm that in polar solvent the state reversal is achieved by intramolecular solvent relaxation. It is also indicated here that twisting of COOH group have no contribution to produce the state reversal. For perpendicular geometry of $N(CH_3)_2$ group, the charge difference on N atom between ground and

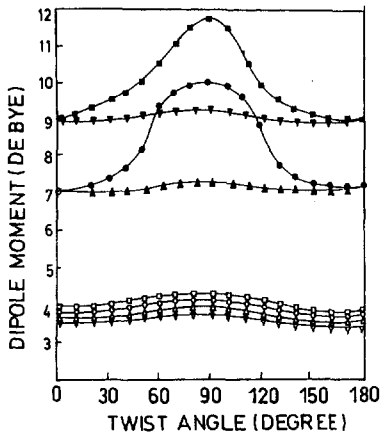

Fig. 9. Variation of excited and ground state dipole moment with different twisted conformations. (– ■ –) COOH in planar position and $N(CH_3)_2$ is twisted in excited state. (– ● –) COOH in perpendicular position and $N(CH_3)_2$ is twisted in excited state. (– ▼ –) $N(CH_3)_2$ in planar position and COOH is twisted in excited state. (– ▲ –) $N(CH_3)_2$ in perpendicular position and COOH is twisted in excited. (– ○ –) COOH in planar position and $N(CH_3)_2$ is twisted in ground state. (– ▽ –) COOH in perpendicular position and $N(CH_3)_2$ is twisted in ground state. (– □ –) $N(CH_3)_2$ in planar position and COOH is twisted in ground state. (– △ –) $N(CH_3)_2$ in perpendicular position and COOH is twisted in ground state.

excited state is ($\Delta q = 0.65$) than that in planar geometry ($\Delta q = 0.1$). So the second excited state ^1A has no doubt a TICT character. The triplet state energy calculations produce the same effect as ^1A state and have slight lower energy (which has also been experimentally observed, vide supra). So singlet and triplet states are nearly degenerate in nature and the charge transfer in all these cases are termed as biradical charge transfer [49].

Fig. 9 depicts the variation of ground and excited state dipole moments with angle of twist of $N(CH_3)_2$ and COOH group keeping COOH group in planar and perpendicular position {for twisting of $N(CH_3)_2$ group} and $N(CH_3)_2$ in planar and perpendicular position (for twisting of COOH group), respectively. In ground state the variation of dipole moment is small for different configurations and the dipole moment has a little value in the perpendicular geometry of both end groups. The excited state dipole moment is always greater than ground state dipole moment. Dependence of excited state dipole moment shows a maximum value for the perpendicular geometry of both the groups. This change of dipole moment ($\Delta\mu = 7.5$ D) corroborates the experimental value 9.23 D and confirms that a major redistribution of charge in excited state takes place which again speaks about TICT nature of charge transfer state.

Now in the light of above quantum chemical calculations the expected mechanism of dual fluorescence of DMACA may be through energetically advantageous intramolecular relaxation involving the twisting of $N(CH_3)_2$ around C–N bond. On excitation, the planar molecule achieves a delocalized excited state and then relaxes to twisted geometry, taking part in charge transfer reaction. Obviously, the emission from twisted conformer will have a large stokes shift and also sensitive to environment effect due to large dipole moment change.

6. Conclusion

Solvent dependent emission spectra help us to conclude the formation of hydrogen bond between DMACA and solvent molecules in favorable environment, and the different characteristics of absorption band in acidic and basic medium reflect the idea of charge transfer character of the molecule. The evidence of the dual fluorescence band in polar media and a probable presence of charge transfer state from absorption spectra point us to probe the intriguing nature of ICT state. Various experimental observations such as emission in different solvents as well as solvent mixture, emission at glass matrices, emission at highly viscous media, polarization study of fluorescence spectra at ambient temperature and at 77 K and lifetime measurements in polar and nonpolar media of fluorescence spectra have confirmed the possibility of formation of TICT state in DMACA. Quantum chemical calculations have also substantiated the idea of TICT state showing maximum dipole moment and low energy of excited state in the twisted geometry (90°) of $N(CH_3)_2$ group. Also it has been established that the rotation of other group COOH has little effect on the energy and dipole moment of TICT state. Ground and excited state dipole moments have been measured and also computed for different twisted geometries. Besides this, low temperature emission confirm the formation of triplet states that are vibronically coupled to each other in hydrocarbon glass. Hence we conclude that twisting of dimethyl amino group coupled with electron transfer from amino nitrogen to the carbonyl group through extended π_z^* of phenyl ring over CH=CH chain. So the introduction of CH=CH chain between phenyl ring and carbonyl group acts as conducting path.

The luminescence and absorption properties of the supramolecular complex between DMACA and β-CD have been studied in the light of probable TICT state. On the basis of the above results and discussion of β-CD inclusion complex we may conclude that the orientation of the TICT fluorophore in the β-CD cavity is the major factor to control the population of TICT excited state and hence the modulation of photophysics.

Acknowledgements

The help rendered by the Chemical Physics group at T.I.F.R., Mumbai and Dr. S. Basak, S.I.N.P., Calcutta in picosecond and nanosecond fluorescence lifetime measurements, respectively, is gratefully acknowledged. The authors wish to thank Mr. Samiran Kar, Department of Organic Chemistry, IACS, Calcutta for synthesizing the sample. Thanks are due to Prof. S.K. Roy for his help in ground state dipole moment measurement. The authors also thank Prof.

P.K. Mukherjee, IACS for making the necessary software available to them and to Dr. Golam Mostafa, IACS for help in calculations.

References

[1] E.M. Kosower, D. Huppert, Annu. Rev. Phys. Chem. 37 (1986) 127.
[2] E. Lippert, W. Luder, H. Boss, in: A. Mangini (Ed.), Advance in Molecular Spectroscopy, Pergamon, Oxford, 1979, p. 443.
[3] K. Rotkiewicz, K.H. Grellmann, Z.R. Grabowski, Chem. Phys. Lett. 19 (1973) 315.
[4] K. Rotkiewicz, Z.R. Grabowski, A. Krowczynski, W. Kuhnle, J. Lumin. 12 (1976) 877.
[5] Z.R. Grabowski, K. Rotkiewicz, W. Rubaszewska, E. Kirkorkaminska, Acta. Phys. Pol. A 54 (1978) 767.
[6] Z.R. Grabowski, K. Rotkiewicz, A. Sicmiarczuk, D.J. Cowley, W. Baumann, Nouv. J. Chim. 3 (1979) 420.
[7] Z.R. Grabowski, K. Rotkiewicz, A. Siemiarczuk, J. Lumin. 18 (1979) 42.
[8] U. Leinhos, W. Kühnle, K.A. Zachariasse, J. Phys. Chem. 95 (1991) 2013.
[9] R.J. Visser, A.G.O. Varma, J. Chem. Soc. Faraday. Trans. 76 (2) (1980) 4531.
[10] R.J. Visser, A.G.O. Varma, J. Konijnenberg, P. Bergwerf, J. Chem. Soc. Faraday. Trans. 79 (2) (1983) 347.
[11] W. Rettig, Narch. Chem. Tech. Lab. 39 (1979) 298.
[12] W. Rettig, Angew. Chem., Int. Ed. Engl. 25 (1986) 971.
[13] K.A. Al-Hassan, W. Rettig, Chem. Phys. Lett. 126 (1986) 273.
[14] W. Rettig, R. Fritz, in: K. Honda (Ed.), Photochemical Processes in Organised Molecular System, Springer, 1991, Elsevier, Amsterdam, p. 61.
[15] W. Rettig, in: O.S. Wolfbeis (Ed.), Fluorescence Spectroscopy, New Methods and Applications, Springer, Berlin, 1993, p. 31.
[16] P. Plaza, N.D. Jung, M.M. Martin, Y.H. Meyer, M. Vogel, W. Rettig, Chem. Phys. 168 (1992) 365.
[17] J.L. Habib Jiwan, J.P. Soumillion, J. Photochem. Photobiol. A: Chem. 64 (1992) 145.
[18] V. Ramamurthy, D.F. Eaton, Acc. Chem. Res. 21 (1988) 300.
[19] P.R. Bangal, S. Lahiri, S. Kar, S. Chakravorti, J. Lumin. 69 (1996) 49.
[20] S.P. Tay, J. Crossley, Can. J. Chem. 50 (1972) 2031.
[21] N. Periasamy, S. Doraiswamy, G.B. Maiya, B. Venkataraman, J. Chem. Phys. 88 (1988) 1638.
[22] H.H. Jaffe, M. Orchin, Theory and Application of Ultraviolet Spectroscopy, Wiley, New York.
[23] S. Gangopadhyay, M. Ali, P. Banerjee, J. Chem. Soc., Perkin Trans. 2 (1992) 781.
[24] M. Windholz (Ed.), The Merck Index, 9th edn., Merck, NJ, USA, 1976, p. 429.
[25] P.R. Bangal, S. Chakravorti, Indian J. Phys. B 70 (1996) 5.
[26] P.R. Bangal, S. Chakravorti, G. Mostafa, J. Photochem. Photobiol. A 113 (1998) 35.
[27] W. Rettig, F. Marschner, Nouv. J. Chim. 7 (1983) 425.
[28] P. Suppan, J. Photochem. Photobiol. A: Chem. 50 (1990) 293.
[29] M.V. Auweraer, Z.R. Grabowski, W. Rettig, J. Phys. Chem. 95 (1991) 2083.
[30] Y.B. Jiang, Appl. Spectrosc. 28 (1986) 1169.
[31] K. Hara, D.S. Bulgarevich, O. Kajimoto, J. Chem. Phys. 104 (1996) 9431.
[32] A. Nag, K. Bhattacharyya, Chem. Phys. Lett. 151 (1988) 474.
[33] A. Nag, K. Bhattacharyya, J. Chem. Soc., Faraday. Trans. 86 (1990) 53.
[34] R.S. Becker, Theory and Interpretation of Fluorescence and Phosphorescence, Wiley Interscience, New York, 1969.
[35] K.K. Rohatgi-Mukherjee, Fundamentals of Photochemistry, Wiley Eastern, New Delhi, 1978.
[36] H. Shizuka, Pure and Appl. Chem. 65 (1993) 1635.
[37] Y. Wang, K.B. Eisenthal, J. Chem. Phys. 77 (1982) 6077.
[38] S.J. Striekler, R.A. Berg, J. Chem. Phys. 37 (1962) 814.
[39] M. Hoshino, M. Imamuro, K. Ikehare, Y. Hama, J. Phys. Chem. 85 (1981) 1820.
[40] Y.B. Jain, Spectrochim. Acta A 51 (1995) 275.
[41] V. Ramamurthy, K. Venkatesan, Chem. Rev. 87 (1987) 433.
[42] A. Nag, R. Dutta, N. Chattopadhyay, K. Bhattacharyya, Chem. Phys. Lett. 157 (1989) 83.
[43] K. Bhattacharyya, M. Chowdhury, Chem. Rev. 93 (1993) 507.
[44] M.J. Smith, K. Krogh-Jespersen, R.M. Levy, Chem. Phys. 171 (1993) 97.
[45] A.C. Testa, J. Lumin. 50 (1991) 243.
[46] J.J. Stewart, MOPAC Program 455, Quantum Chemistry Program Exchange, University of Indiana, Bloomington, IN.
[47] M.J.S. Dewar, E.G. Zoebisch, E.F. Healy, J.J. Stewart, J. Am. Chem. Soc. 107 (1985) 3902.
[48] M.J.S. Dewar, W. Thiel, J. Am. Chem. Soc. 99 (1977) 4899.
[49] V. Bonacic-Koutecky, J. Michl, J. Am. Chem. Soc. 107 (1977) 1765.